Multi-Operator Spectrum Sharing for Massive IoT Coexisting in 5G/B5G Wireless Networks

Bo Qian, *Student Member, IEEE*, Haibo Zhou, *Senior Member, IEEE*, Ting Ma, *Student Member, IEEE*, Kai Yu, *Student Member, IEEE*, Quan Yu, *Senior Member, IEEE*, and Xuemin Shen, *Fellow, IEEE*

***Abstract*— With a massive number of Internet-of-Things (IoT) devices connecting with the Internet via 5G or beyond 5G (B5G) wireless networks, how to support massive access for coexisting cellular users and IoT devices with quality-of-service (QoS) guarantees over limited radio spectrum is one of the main challenges. In this paper, we investigate the multi-operator dynamic spectrum sharing problem to support the coexistence of rate guaranteed cellular users and massive IoT devices. For the spectrum sharing among mobile network operators (MNOs), we introduce a wireless spectrum provider (WSP) to make spectrum trading with MNOs through the Stackelberg pricing game. This framework is inspired by the active radio access network (RAN) sharing architecture of 3GPP, which is regarded as a promising solution for MNOs to improve the resource utilization and reduce deployment and operation cost. For the coexistence of cellular users and IoT devices under each MNO, we propose the coexisting access rules to ensure their QoS and the priority of cellular users. In particular, we prove the uniqueness of the Stackelberg equilibrium (SE) solution, which can maximize the payoffs of MNOs and WSP simultaneously. Moreover, we propose an iterative algorithm for the Stackelberg pricing game, which is proved to achieve the unique SE solution. Extensive numerical simulations demonstrate that, the payoffs of WSP and MNOs are maximized and the SE solution can be reached. Meanwhile, the proposed multi-operator dynamic spectrum sharing algorithm can support more than almost 40% IoT devices compared with the existing no-sharing method, and the gap is less than about 10% compared with the exhaustive method.**

***Index Terms*— 5G/B5G, IoT devices, cellular users, spectrum sharing, Stackelberg pricing game, massive access.**

I. Introduction

WITH the significant development of wireless networks, tens of billions of Internet-of-Things (IoT) devices will access the next-generation mobile communication networks, i.e., fifth generation (5G) or beyond 5G (B5G), for realizing advanced applications, such as smart city management, unmanned environmental monitoring and collaborative Intelligent Transportation Systems (ITS) [1]–[5]. According to the recent 5G IoT report [6], up to 20.8 billion IoT devices will be in use worldwide by 2020 and the IoT market will grow to over 3 trillion annually by 2026, which is due to increased industry focus and the IoT technologies from the third-generation partnership project (3GPP) standardization.

As the access number of IoT devices explodes in 5G/B5G wireless networks, one main challenge for mobile network operators (MNOs) lies in accommodating the fast-growing traffic services generated by both high-speed cellular users and massive IoT devices over limited radio spectrum, considering the quality-of-service (QoS) guarantees and cost issues [7], [8]. Recent research [9] reports that, for a typical European cellular operator, network sharing could reduce more than 50% of infrastructure cost in 5G deployment. In Release 14 [10], 3GPP proposed a novel radio access network (RAN) sharing architecture named active RAN sharing, in which a master operator was designated as the only entity to manage the resource shared among the participating operators. Despite its great potential, the network sharing would significantly increase the implementation complexity of wireless systems for multiple MNOs. How to quickly access a large number of cellular users coexisting with massive IoT devices and allocate the required spectral bandwidth for them in a multi-operator spectrum sharing architecture is still an open problem [11].

Different from conventional spectrum sharing among cellular users, there are two main characteristics for the spectrum sharing of massive IoT devices in 5G/B5G wireless networks. The first characteristic lies in the traffic model, i.e., conventional spectrum sharing technologies are mainly developed for downlink long-packet communications from a base station (BS) to mobile devices. However, the future spectrum sharing of IoT devices in 5G/B5G wireless networks will be dominated by uplink short-packet communications from end devices (EDs) to the BS, which requires the scheme design of spectrum sharing of massive IoT devices to consider the realtime massive uplink traffic distribution [12]. The second characteristic lies in the IoT device class, i.e., the massive IoT devices are expected to be cheap and thus usually have limited signal-processing capabilities and un-rechargeable batteries. This difference requires simple and efficient scheme design for IoT spectrum sharing to reduce both the scheme computing complexity and energy consumption at EDs. Based on

Manuscript received February 1, 2020; revised June 9, 2020; accepted July 18, 2020. Date of publication August 24, 2020; date of current version February 17, 2021. This work was supported in part by the National Natural Science Foundation of China under Grant 61871211, in part by the Natural Science Foundation Jiangsu Province Youth Project under Grant BK20180329, in part by the Innovation and Entrepreneurship of Jiangsu Province High-Level Talent Program, in part by the Summit of the Six Top Talents Program Jiangsu Province, and in part by the Natural Sciences and Engineering Research Council of Canada (NSERC). *(Corresponding author: Haibo Zhou.)*

Bo Qian, Haibo Zhou, Ting Ma, and Kai Yu are with the School of Electronic Science and Engineering, Nanjing University, Nanjing 210023, China (e-mail: boqian@smail.nju.edu.cn; haibozhou@nju.edu.cn; majiawan27@163.com; kaiyu@smail.nju.edu.cn).

Quan Yu is with the School of Electronic Science and Engineering, Nanjing University, Nanjing 210023, China, and also with the Peng Cheng Laboratory, Shenzhen 518000, China (e-mail: yuquan61@qq.com).

Xuemin Shen is with the Department of Electrical and Computer Engineering, University of Waterloo, Waterloo, ON N2L 3G1, Canada (e-mail: sshen@uwaterloo.ca).

Color versions of one or more of the figures in this article are available online at https://ieeexplore.ieee.org.

Digital Object Identifier 10.1109/JSAC.2020.3018803

above considerations, we investigate a multi-operator spectrum sharing problem to support the coexistence of cellular users and massive IoT devices with guaranteed QoS. Inspired by the active RAN sharing architecture of 3GPP, we introduce a wireless spectrum provider (WSP), as the only third party designated by MNOs, to manage the shared spectrum pool. Due to the scarcity of radio spectrum resources, we adopt the market-based pricing scheme to achieve effective and fair resource allocation [13]. Hence, we propose a Stackelberg pricing game to formulate the spectrum trading between the WSP and MNOs, which can incorporate the cyclic dependency between the bandwidth purchase problems of MNOs and the unit bandwidth pricing of the WSP. Specifically, the leader (i.e., WSP) can maximize its payoff by adjusting the bandwidth price, and the followers (i.e., MNOs) dynamically adjust the amount of required bandwidth to maximize their payoffs, which are based on the bandwidth price and the service fees from cellular users and IoT devices. In order to guarantee the access priority of cellular users as well as the QoS of cellular users and IoT devices, we propose the coexisting access rules. Due to the simplicity of IoT devices, we introduce a truncated channel inversion power control scheme for the EDs, which is usually used in massive IoT networks [14], [15]. Furthermore, we propose an iterative algorithm for the Stackelberg pricing game, which is proven to quickly achieve the Stackelberg equilibrium, i.e., a spectrum sharing agreement including an optimal bandwidth price for the WSP and bandwidth allocation plans for MNOs.

We highlight the novelty and contributions compared with the previous works in three-fold:

- *Stackelberg pricing game framework:* We propose a Stackelberg pricing game framework for spectrum pricing, spectrum sharing, and coexisting access. The framework consists of a unit bandwidth pricing control for the leader (i.e., WSP) and the required bandwidth optimization for followers (i.e., MNOs), which solves the spectrum trading problem between the WSP and MNOs in the coexisting access scenario of cellular users and IoT devices.
- *Optimal spectrum allocation and coexisting access rules:* To quickly achieve a spectrum sharing agreement, we propose an iterative algorithm for the Stackelberg pricing game to optimize the payoffs of the WSP and MNOs. To solve the coexistence problem of cellular users and IoT devices, we propose coexisting access rules and analyze their transmission rates using stochastic geometry techniques.
- *Theoretical proof and optimality:* We prove the existence and uniqueness of the equilibrium point for the Stackelberg pricing game. The proposed algorithm is shown to converge to the equilibrium solution from a theoretical point of view.

The remainder of the paper is organized as follows. Section II reviews the related works. Section III describes the system model and spectrum sharing framework. Section IV provides the performance analysis. Section V and Section VI introduce the Stackelberg pricing game formulation and solution, respectively. Section VII presents the simulation results. Section VIII concludes the paper. In addition, a list of important symbols in the paper is shown in Table I.

TABLE I
SUMMARY OF IMPORTANT SYMBOLS

Parameter	Meaning
B^{req}	Total required spectral bandwidth of MNOs for accessing all cellular users and IoT devices.
B^{max}	Maximum spectral bandwidth owned by the WSP.
B^{tol}	Total marketable spectral bandwidth of the WSP.
B_m	Required spectral bandwidth of MNO m.
$\mathcal{M}$	Set of MNOs under the WSP.
P	Price of bandwidth charged by WSP.
$P_c,\ P_I$	Price for accessing a cellular user and an IoT device.
$\eta_c,\ \eta_r$	Path-loss exponent of cellular users and IoT devices.
$\rho_c,\ \rho_r$	Receive power of cellular users and IoT devices.
$h,\ W_0$	Fading gain and noise power.
$k,\ F$	Number of candidates and total subchannels.
$\tau_{c,0}$	Average rate of cellular users without IoT devices.
$\tau_c,\ \tau_r$	Average rate of cellular users and IoT devices.
$R_{c,0},\ R_{I,0}$	Rate threshold of cellular users and IoT devices.
$U_m,\ U_w$	Payoff of MNO m and the WSP.
$N_{m,c},\ N_{m,c}^{tol}$	Access and total number of cellular users in MNO m.
$N_{m,I},\ N_{m,I}^{tol}$	Access and total number of IoT devices in MNO m.

II. RELATED WORKS

Recently, multi-operator network sharing has gradually become a consensus. In 3GPP Release 10, the concept of network sharing was first introduced to allow multiple MNOs to share their physical networks. The early development of network sharing was referred to as passive RAN sharing [10], which mainly focused on the infrastructure sharing of multiple MNOs. In Release 14, 3GPP introduced a new architecture named active RAN sharing, in which multiple MNOs can share their spectrum resources and core network equipments based on a network sharing protocol, including mutual agreements on legal, financial, and joint operations. Dynamic spectrum sharing, as a technology proposed in 3GPP Release 15, allowed the deployment of both 4G long term evolution (LTE) and 5G new radio (NR) in the same frequency band, and dynamically allocated spectrum resources between the two technologies based on user demands for MNOs.

Moreover, wireless network virtualization is also regarded as an emerging network paradigm to enable sharing of infrastructure and radio spectrum resources, and reduce overall expenses of wireless network deployment and operation [16]. It consists of four main components, i.e., radio spectrum resource, wireless network infrastructure, wireless virtual resource, and wireless virtualization controller. In [17], the authors reviewed 3GPP's network sharing standardized functionality, and concluded that future mobile networks will increasingly involve advanced virtualization solutions, opening the market to a wide range of new business models. In [18], Danda *et al.* formulated a three-layer game for wireless infrastructure providers, mobile virtual network operators, and IoT devices (or end users). Furthermore, in [19], the authors proposed an iterative algorithm for the three-layer game model and analyzed the uniqueness of the equilibrium point. How to design fast and efficient algorithms for the spectrum sharing massive IoT

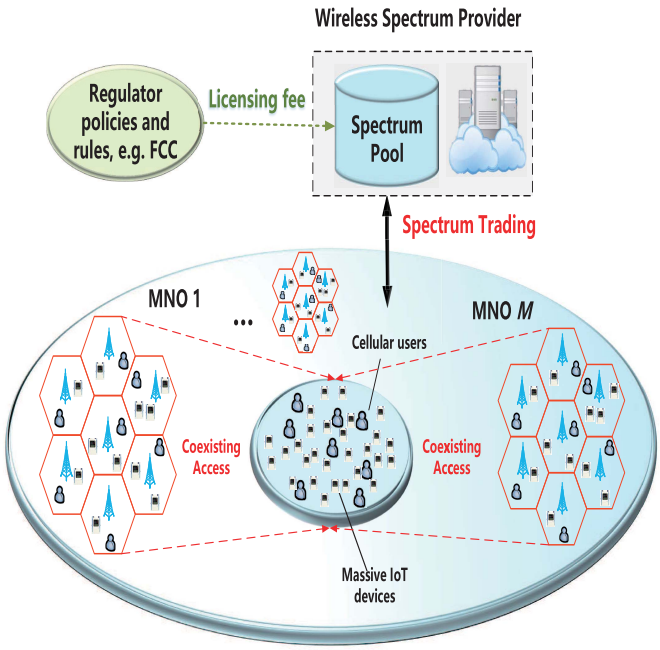

Fig. 1. A multi-operator dynamic spectrum sharing scenario with coexisting access of cellular users and massive IoT devices.

devices, where the user demands change in real time, is still an issue.

Recently, there are also some starting researches on spectrum sharing of multiple operators [20]–[22]. In [23], Yu *et al.* introduced a fully-decoupled RAN architecture for 6G inspired by neurotransmission, in which multiple MNOs in the local area can trade spectrum in real time through the proposed Cybertwin-aided transmission service. In [24], Xiao *et al.* proposed a spectrum pooling system with both primary users and secondary users, and developed a hierarchical game theoretic model for them. In [25], the authors introduced a multi-operator network sharing framework that supports the coexistence of IoT devices and high-speed cellular services. However, how to quickly realize the multi-operator dynamic spectrum sharing with coexisting access of cellular users and massive IoT devices has not been studied. Zhai *et al.* [26] jointly solved user scheduling and power control to investigate the access delay minimization problem for the uplink non-orthogonal multiple access (NOMA) networks with massive IoT devices. Moussa and Zhuang [27] presented a novel NOMA-enabled two-stage transmission architecture for massive cellular IoT communications. They jointly exploited queuing theory and stochastic geometry to derive tractable models under different network parameters. In [28], Singh *et al.* designed a coordination protocol acting on the level of the RAN. The non-cooperative protocol was applicable when the operators formed a spectrum pool and mutually rented spectrum based on a set of negotiation rules.

III. System Model and Spectrum Sharing Framework

We investigate a multi-operator dynamic spectrum sharing scenario that supports the coexistence of cellular users and massive IoT devices. As shown in Fig. 1, we assume that there are M MNOs controlling their own BSs in a local area. Within the coverage of each MNO, cellular users and IoT devices simultaneously use the licensed frequency band for uplink transmission. A WSP, as the only third party, is designated by MNOs to manage the shared spectrum pool, who does not directly lease out its spectrum to the end users. The detailed multi-operator dynamic spectrum sharing scenario is introduced as follows:

- *Spectrum Pool*: The WSP, as a spectrum pool manager, can merge all the spectrum of MNOs to form a common pool for these shared MNOs to use.
- *Spectrum Trading*: The spectrum of these M MNOs is controlled by the WSP, who can trade the spectral bandwidths in real time through spectrum trading.
- *Coexisting Access Rules*: Each cellular user adopts orthogonal subchannels without affecting each other, and the IoT device randomly multiplexes some subchannels for transmission. These cellular users and IoT devices can access the networks and be charged by the MNOs only if their transmission rates exceed a certain threshold, respectively. Additionally, each MNO gives access priority to cellular users, and then considers IoT devices.

A. Network Model

Let the required spectral bandwidth of MNO m be B_m for $m \in \mathcal{M}$ and the maximum spectral bandwidth owned by the WSP be B^{max}. It is easy to see that, when there are a few cellular users and IoT devices under the MNOs, the WSP cannot sell out its all spectral bandwidth B^{max}. Denote B^{req} as the total required spectral bandwidth for accessing all cellular users and IoT devices under the MNOs. Then, we define $B^{tol} \triangleq \min\{B^{req}, B^{max}\}$ as the total marketable spectral bandwidth for the WSP. In the spectrum trading, denote P as the price charged by WSP for each MNO (i.e., usage fee in \$ per unit of bandwidth). Considering the heterogeneity of services, i.e., different QoS requirements, the two classes of EDs (i.e., cellular users and IoT devices) should be charged at different prices. Meanwhile, taking into account the fairness of the system, we assume that each MNO charges the services under a uniform charging standard. Hence, we denote P_c and P_I as the access prices charged by MNOs for each cellular user and IoT device, respectively (i.e., fixed access fee in \$ per user per unit of time). Moreover, when the budget of each cellular user or IoT device is not enough to support the communication cost, MNOs can reject the communication request until it submits a more sufficient budget.

Since massive IoT devices usually only have uplink transmission, such as enhanced machine-type communication (eMTC) [29], we consider the massive access problem of IoT devices coexisting with cellular users in the uplink transmission system. As usually used in IoT networks [14], [15], we apply a full path-loss inversion power control at all IoT devices to solve "near-far" problem, where each IoT device controls its transmit power by compensating for its own path-loss to maintain the average received signal power in the BS equaling to a same threshold ρ. In our framework,

the transmission powers of cellular users and IoT devices are regulated by the truncated channel inversion power control model, which is widely used in the uplink transmission [30], [31], i.e., the received signal power is required to equal a certain receive power threshold $\rho_i,\ i = c, r$, for cellular users and IoT devices, respectively. Once the user or device is too far away from the BS to keep the average received signal power equal to the prescribed threshold, the communication request will be interrupted by the MNOs, which is called the truncation outage. Only requests sent from cellular users and IoT devices that reach the specified receive power and budget constraint are considered as legitimate communication requests by MNOs.

B. Transmission and Channel Model

We investigate a general power-law path-loss model with the decay rate $d^{-\eta}$, where d indicates the distance between transmitter and receiver, and $\eta > 2$ represents the path-loss exponent. In particular, we denote η_c and η_r as the path-loss exponents of cellular users and IoT devices, respectively. According to the aforementioned truncated channel inversion power control, the received signal power is $\rho_i,\ i = c, r$, for cellular users and IoT devices, respectively. Hence, we can express the received power as $\rho_i h$, with h being the channel gain. Here, we consider a Rayleigh fading channel and $h \sim \exp(1)$ [32].

Suppose that the available spectral bandwidth for the BS of MNO $m \in \mathcal{M}$ consists of F subchannels, each of which has spectral bandwidth $\frac{B_m}{F}$. Meanwhile, the cellular users and IoT devices have different spectrum allocation schemes, which are usually introduced in cellular LTE networks [33]. For the cellular users, we assume that the BS schedules the spectrum resources in a round-robin (RR) manner, which results in an equal sharing of spectrum resources for these users. For the IoT devices, each one randomly chooses k out of F subchannels as candidates and accesses each of the k subchannels with probability p_m, which means that it can multiplex multiple subchannels simultaneously for transmission. Based on this allocation scheme, the probability of selecting the subchannel $l \in \{F\}$ as a candidate is $p_l = \frac{C_F^k - C_{F-1}^k}{C_F^k} = \frac{k}{F}$ and the access probability is $p_l p_m$.

C. A Dynamic Spectrum Sharing Framework in 5G/B5G

In the light of [33], we propose a dynamic spectrum sharing framework, which is composed of two levels: the MNOs (followers) required bandwidth optimization and the WSP (leader) unit bandwidth pricing control, as shown in Fig. 2.

1) *Required Bandwidth Optimization for the Followers:* Each MNO chooses an optimal amount of required bandwidth based on its utility maximization, which jointly considers the bandwidth price and its own load conditions (i.e., the numbers of cellular users and IoT devices), and feeds it back to the WSP. According to the coexisting access rules, the MNOs preferentially access the cellular users, who can be charged at price P_c only if the transmission rate is larger than threshold $R_{c,0}$. For IoT devices, they are allowed to randomly multiplex channels only after cellular users are all connected.

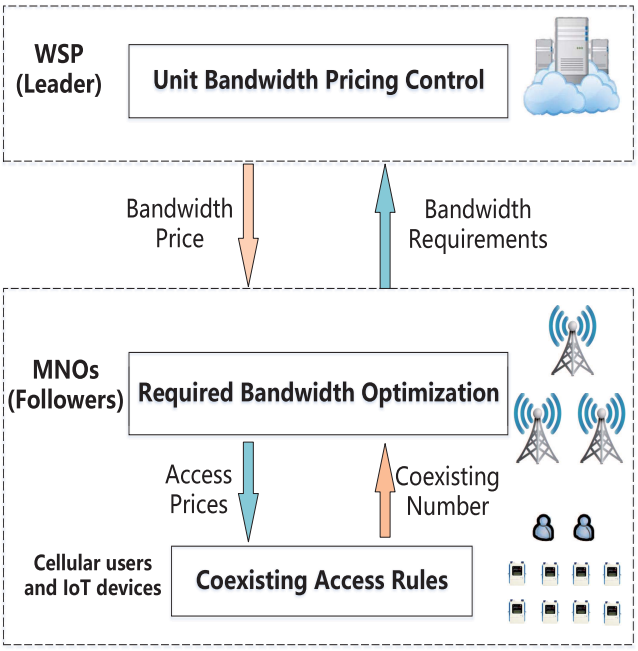

Fig. 2. A Stackelberg pricing game framework for pricing, spectrum sharing, and coexisting access.

It will be charged at price P_I when the transmission rate exceeds threshold $R_{I,0}$. Thus, the MNOs first publish the rate thresholds and access prices. Then, the cellular users and IoT devices determine whether to send access requests. Subsequently, the MNOs can solve the required bandwidth optimization problems based on their own loads.

2) *Unit Bandwidth Pricing Control for the Leader:* In order to allocate the spectrum resources reasonably, WSP conducts spectrum trading with MNOs through controlling the unit bandwidth price P. After collecting all feedbacks from MNOs, the WSP develops an optimal bandwidth price based on its own benefit maximization.

Hence, we apply a Stackelberg pricing game to model the dynamic pricing of WSP and dynamic spectrum sharing of MNOs. Meanwhile, we use the backward induction to analyze the Stackelberg equilibrium solution.

IV. Performance Analysis

Note that, the authorized frequency bands of MNOs are orthogonal. When each MNO deploys its own BSs, neighbouring BSs are assigned different groups of channels in cellular system, which leads to independency of BSs with each other in a local area. Then, the bandwidth requirement amount of the MNO is the sum of its all BSs' required bandwidth. Therefore, we only analyze the situation that each MNO controls one BS. In this section, we take MNO m as an example to conduct performance analysis because the access model of cellular users and IoT devices are the same for each MNO. Considering that the future spectrum sharing of IoT devices in 5G/B5G wireless networks will be dominated by uplink short-packet communications from EDs to the BS, we need to remodel and analyze the traffic distributions of uplink transmission and multiplexing. According to the coexisting access rules, we first

analyze the transmission rates of cellular users and IoT devices in two cases, i.e., coexisting and not coexisting with IoT devices. Then, we formulate the optimization problems about the maximum access numbers of cellular users and coexisting IoT devices.

A. Average Transmission Rate of Cellular Users When Not Coexisting With IoT Devices

For the case of no coexisting with IoT devices, there is no interference for the transmission of cellular users. The signal-to-noise ratio (SNR) of the receiver can be represented as:

$$\text{SNR}_c^l = \frac{P_u h_c d_c^{-\eta_c}}{W_0} = \frac{\rho_c h_c}{W_0},$$

where P_u is the transmit power of cellular users, h_c is the fading gain from its transmitter to the receiver and W_0 denotes the noise power. Using the techniques in stochastic geometry [33], we can obtain the following result.

Proposition 1: The average spectrum efficiency of a cellular user without IoT devices coexisting is given by

$$\bar{\tau}_{c,0} = \frac{1}{\ln 2} \exp\left\{\frac{W_0}{\rho_c}\right\} E_1\left(\frac{W_0}{\rho_c}\right),$$

where $E_1(x) = \int_x^\infty \frac{e^{-t}}{t} dt$ is the exponential integral.

Proof: See Appendix A. ∎

Note that, for the cellular users not coexisting with IoT devices, the BS schedules the spectrum resources in a RR manner and the probability for a user to be allocated a subchannel l is $\frac{1}{N_c}$, where N_c is the number of users under the BS. Thus, the average spectral bandwidth allocated to a cellular user is derived as:

$$B_{m,c} = \sum_{l=1}^{F} \frac{B_m}{F} \cdot \frac{1}{N_c} = \frac{B_m}{N_c}.$$

Correspondingly, when not coexisting with IoT devices, the average transmission rate of a cellular user is $\tau_{c,0}^m = B_{m,c}\bar{\tau}_{c,0}$.

B. Average Transmission Rate of Cellular Users When Coexisting With IoT Devices

Since this paper considers the spectrum sharing among multiple MNOs in a local area, there is no interference among BSs because of the orthogonal spectrum division. Denote N_c and N_I as the numbers of cellular users and IoT devices under the BS, respectively. When a cellular user accesses the subchannel l, the interference comes from other IoT devices reusing the same subchannel l in Φ_r^l. It should be noted that the BS is the receiver of all cellular users and IoT devices. Then, the aggregate interference suffered by the receiver is:

$$I_c^l = \sum_{X_i \in \Phi_r^l} P_r h_r d_r^{-\eta_r},$$

where P_r is the transmit power of IoT device X_i, h_r denotes the fading gain from X_i to the BS, and d_c represents the distance from X_i to the BS. Similar to [30], we make the following assumption to maintain the model tractability.

Assumption 1: The cellular users and IoT devices using the same uplink subchannel are independent in spatial distributions.

In this case, the signal-to-interference-plus-noise ratio (SINR) of the receiver can be represented as follows:

$$\text{SINR}_c^l = \frac{P_u h_c d_c^{-\eta_c}}{I_c^l + W_0} = \frac{\rho_c h_c}{I_c^l + W_0}.$$

After getting the SINR, we can draw the following conclusion based on the Shannon's formula.

Proposition 2: The average spectrum efficiency of a cellular user coexisting with IoT devices is given by

$$\bar{\tau}_c = \frac{1}{\ln 2} \int_0^\infty \frac{1}{v+1} e^{-\frac{W_0}{\rho_c} v} \left(\frac{\rho_c}{v\rho_r + \rho_c}\right)^{N_I p_m p_l} dv.$$

Proof: See Appendix B. ∎

Since the BS schedules the spectrum resources for cellular users in the same manner with the case of no IoT devices, the allocated spectral bandwidth for the cellular users is also $B_{m,c} = \frac{B_m}{N_c}$. Correspondingly, the average transmission rate of the cellular users is $\tau_c^m = B_{m,c}\bar{\tau}_c$.

C. Average Transmission Rate of IoT Devices When Coexisting With Cellular Users

For an IoT device reusing a subchannel l, the interferers are the cellular user in subchannel l (denoted as I_{cr}^l) and other IoT devices reusing the same subchannel l (denoted as I_{rr}^l). Then, the overall interference suffered by the IoT device in subchannel l could be expressed as follows:

$$\begin{aligned} I_r^l &= I_{cr}^l + I_{rr}^l = P_u h_c d_c^{-\eta_c} + \sum_{X_i \in \Phi_{rr}^l} P_r h_r d_r^{-\eta_r} \\ &= \rho_c h_c + \sum_{X_i \in \Phi_{rr}^l} \rho_r h_r. \end{aligned}$$

Correspondingly, we could derive the SINR of the IoT device as follows:

$$\text{SINR}_r^l = \frac{P_r h_r d_r^{-\eta_r}}{I_r^l + W_0} = \frac{\rho_r h_r}{I_r^l + W_0},$$

where h_r is the fading gain from the transmitter to its receiver, d_r represents the distance between the IoT device and the BS.

Similar to the analysis for the cellular users, the average spectrum efficiency for an IoT device coexisting with cellular users is given as follows.

Proposition 3: The average spectrum efficiency of an IoT device coexisting with cellular users is given by

$$\bar{\tau}_r = \frac{1}{\ln 2} \int_0^\infty e^{-\frac{W_0}{\rho_r} v} \frac{\rho_r}{v\rho_c + \rho_r} \left(\frac{1}{v+1}\right)^{N_I p_m p_l} dv.$$

Proof: See Appendix C. ∎

On the basis of the resource allocation schemes, the average spectral bandwidth allocated to an IoT device is $B_{m,r} = \frac{k p_m B_m}{F}$. Hence, the average transmission rate of the IoT devices could be derived as $\tau_r^m = B_{m,r}\bar{\tau}_r$.

D. Number of Cellular Access Users When Not Coexisting With IoT Devices

After getting the average rates of cellular users and IoT devices, we can derive the relationship between allocated spectral bandwidth and the maximum number of coexisting IoT devices.

First, when the spectral bandwidth B_m is scarce for MNO m, the MNO preferentially guarantees the access of cellular users. In this case, without the interference of IoT devices, we can derive the average rate $\tau_{c,0}^m$ of cellular users in MNO m according to *Proposition 1*. Denote $\mathbb{N}$ as the positive integer field and $N_{m,c} \in \mathbb{N}$ is the number of cellular access users for MNO m. Hence, with a given spectral bandwidth B_m, the maximum number of cellular access users can be obtained by solving the following problem:

$$\begin{aligned} \max_{N_{m,c}} \quad & N_{m,c} \\ \text{s.t.} \quad & \tau_{c,0}^m \geq R_{c,0},\ 0 \leq N_{m,c} \leq N_{m,c}^{tol},\ N_{m,c} \in \mathbb{N}, \end{aligned} \tag{1}$$

where $R_{c,0}$ is the required rate for cellular users, and $N_{m,c}^{tol}$ is the total cellular users who require communications in MNO m. Through solving problem (1), we can get the maximum number of cellular access users as $N_{m,c}^{\max}(B_m)$. Obviously, the larger the spectral bandwidth B_m, the more cellular users can access. Thus, for (1), there is a spectral bandwidth $B_{m,0}$ that just satisfies all cellular users, while the corresponding rate just reaches the threshold $R_{c,0}$.

E. Coexisting Number of Cellular Users and IoT Devices

For the case of sufficient spectral bandwidth, after all cellular users are served, MNO m begins to consider the access of IoT devices. We can derive the average rate τ_c^m and τ_r^m of cellular users and IoT devices in MNO m according to *Proposition 2* and *Proposition 3*, respectively. In order to guarantee the QoS of cellular users and IoT devices, their average rates are required to exceed thresholds $R_{c,0}$ and $R_{I,0}$, respectively. Since the BS is assumed to preferentially guarantee the access of cellular users, in the case of known spectral bandwidth B_m, the maximum number of coexisting IoT devices can be obtained by solving the following problem:

$$\begin{aligned} \max_{N_{m,I}} \quad & N_{m,I} \\ \text{s.t.} \quad & \tau_c^m \geq R_{c,0}, \qquad \tau_r^m \geq R_{I,0}, \\ & 0 \leq N_{m,I} \leq N_{m,I}^{tol}, \qquad N_{m,I} \in \mathbb{N}, \end{aligned} \tag{2}$$

where $N_{m,I}^{tol}$ is the total number of IoT devices requiring communications under MNO m. Via solving problem (2), we can get the maximum number of coexisting IoT devices as $N_{m,I}^{\max}(B_m)$.

V. Stackelberg Pricing Game Formulation

After deriving the performance analysis of access cellular users and IoT devices in the cases of scarce and sufficient spectral bandwidths, we first establish the utility definition of WSP and MNOs, respectively. In order to incorporate the dynamics of WSP and MNOs, we then formulate a Stackelberg pricing game where the WSP is the leader and the MNOs are followers, and formulate optimization problems to maximize corresponding payoffs in each layer.

A. Payoff Maximization Sub-Game of WSP

Definition 1 (WSP Utility): Government bodies, such as the Federal Communications Commission (FCC) in the US, assign spectrum to WSP and collect licensing fees from WSP. The WSP subleases its licensed spectrum to MNOs through spectrum trading. Similar to [19], with given unit bandwidth price P and required spectral bandwidth B_m of MNO m, the utility of the WSP is quantified as follows:

$$U_w = r_m - C = \frac{P}{2} \cdot \left(\min\{ \sum_{m=1}^{M} B_m, B^{tol} \} \right)^2 - C, \tag{3}$$

where r_m represents the payment charged from MNOs with a unit bandwidth price P, and C is the licensing cost paid to the regulatory agency, such as the FCC.

Layer 1: The Sub-Game of Leader: The WSP offers its optimal price for its licensed spectrum to attract more MNOs with an aim of maximizing its utility. The WSP strategically chooses the pricing P by solving the WSP payoff maximization sub-game (WPMS):

$$\begin{aligned} \max_{P} \quad & U_w(P) = \frac{P}{2} \cdot \left(\min\{ \sum_{m=1}^{M} B_m^*(P), B^{tol} \} \right)^2 - C \\ \text{s.t.} \quad & P \geq 0, \end{aligned} \tag{4}$$

where $B_m^*(P)$ is the optimal bandwidth requirement of MNO m with a given price P.

B. Payoff Maximization Sub-Game of MNOs

Definition 2 (MNOs Utility): As previous arguments, each MNO charges the access of cellular users and IoT devices according to the coexisting access rules. For MNO m, when the spectral bandwidth $B_m \leq B_{m,0}$, only cellular users can be served and the maximum number is $N_{m,c}^{\max}$ through solving problem (1). When the spectral bandwidth $B_m > B_{m,0}$, IoT devices can be served coexisting with cellular users and the maximum number of IoT devices is $N_{m,I}^{\max}$ through solving problem (2). Assuming the total number of cellular users is $N_{m,c}^{tol}$, with a given bandwidth price P, the payoff of MNO m can be expressed as the payment charged from its users minus the spectral bandwidth payment paid to the WSP:

$$U_m = \begin{cases} P_c \cdot N_{m,c}^{\max} - \dfrac{P}{2} \cdot B_m^2, & \text{for } B_m \leq B_{m,0}, \\ P_c \cdot N_{m,c}^{tol} + P_I \cdot N_{m,I}^{\max} - \dfrac{P}{2} \cdot B_m^2, & \text{for } B_m > B_{m,0}, \end{cases} \tag{5}$$

where P_c and P_I represent the price per user for cellular users and IoT devices, respectively.

Layer 2: The Followers Sub-Game: In this sub-game, each MNO tries to submit suitable bandwidth requirement to maximize its payoff based on the announced price P by the WSP and its own load condition. Hence, the MNOs

payoff maximization sub-game (MPMS) is formulated as the following three tuples:

$$\text{MPMS} = \langle \mathcal{M}, \{S_m\}_{m\in\mathcal{M}}, \mathcal{U}_m(\cdot)\rangle,$$

where $\mathcal{M} = \{1, 2, \cdots, M\}$ is the set of MNOs who are the players in layer-2 sub-game, S_m is the set of actions that the player could take, i.e., the required bandwidth of MNO m, and $\mathcal{U}_m(\cdot)$ is the payoff that maps the outcome for a chosen action of player MNO m.

Considering the coexisting access rules for cellular users and IoT devices, we can calculate $B_{m,0}$ as the smallest bandwidth of MNO m for accessing all cellular users. Then, we have two situations for the MPMS, i.e., the scarce bandwidth situation ($B_m \le B_{m,0}$) and sufficient bandwidth situation ($B_m > B_{m,0}$), which are named MPMS-1 and MPMS-2, respectively. For the scarce bandwidth situation, we have the following MPMS-1:

$$\begin{aligned} \max_{B_m} \quad & U_{1,m}(B_m) = P_c \cdot N_{m,c}^{\max}(B_m) - \frac{P}{2}\cdot B_m^2 \\ \text{s.t.} \quad & B_m \le B_{m,0}, \end{aligned} \tag{6}$$

where $N_{m,c}^{\max}(B_m)$ is the optimal solution of problem (1) for a given bandwidth B_m. In the following, we denote the optimal solution of MPMS-1 as $B_{1,m}^*$, $N_{m,c}^* \triangleq N_{m,c}^{\max}(B_{1,m}^*)$, and $U_{1,m}^* \triangleq U_{1,m}(B_{1,m}^*)$.

Similarly, for the case of sufficient bandwidth, MPMS-2 can be formulated as:

$$\begin{aligned} \max_{B_m} \quad & U_{2,m}(B_m) = P_c \cdot N_{m,c}^{tol} + P_I \cdot N_{m,I}^{\max}(B_m) - \frac{P}{2}\cdot B_m^2 \\ \text{s.t.} \quad & B_m > B_{m,0}, \end{aligned} \tag{7}$$

where $N_{m,c}^{tol}$ is the total number of cellular users under MNO m, and $N_{m,I}^{\max}(B_m)$ is the maximum coexisting number of IoT devices for a given bandwidth B_m by solving problem (2). In the following, we denote the optimal solution of MPMS-2 as $B_{2,m}^*$, $N_{m,I}^* \triangleq N_{m,I}^{\max}(B_{2,m}^*)$, and $U_{2,m}^* \triangleq U_{2,m}(B_{2,m}^*)$.

Then, we can obtain the optimal required spectral bandwidth B_m^* of MPMS by comparing $U_{1,m}^*$ and $U_{2,m}^*$.

VI. Solution and Unique Equilibrium

Since the payoffs of MNOs rely on the bandwidth price announced by the WSP, we use the backward induction approach to find the equilibrium solution. We first solve the optimal strategy of MNOs in Layer-2 sub-game. Then, we use the optimal solution of MNOs to find the best pricing strategy of WSP in Layer-1 sub-game. Finally, we show the existence of equilibrium point in the Stackelberg pricing game.

A. Optimal Solution for MPMS-1 of MNOs

When the required spectral bandwidth keeps growing from zero, more and more cellular users can be served. As $B_{m,0}$ is the smallest spectral bandwidth for MNO m to access all $N_{m,c}^{tol}$ cellular users, we can deduce that $B_{m,0}$ is the spectral bandwidth that enables the rates of all cellular users just meet the threshold $R_{c,0}$.

Lemma 1: The solution of problem (1) is $N_{m,c}^{\max} = \frac{B_m \exp\{\frac{W_0}{\rho_c}\} E_1(\frac{W_0}{\rho_c})}{\ln 2 \cdot R_{c,0}}$, for $B_m \le B_{m,0}$.

Proof: From *Proposition 1*, the average transmission rate of a cellular user without IoT devices coexisting is:

$$\tau_{c,0}^m = B_c \bar{\tau}_{c,0} = \frac{B_m}{N_{m,c}} \frac{1}{\ln 2} \exp\left\{\frac{W_0}{\rho_c}\right\} E_1\left(\frac{W_0}{\rho_c}\right),$$

where $E_1(x) = \int_x^\infty \frac{e^{-t}}{t} dt$. When accessing all cellular users in MNO m (i.e., $N_{m,c} = N_{m,c}^{tol}$), we can derive the spectral bandwidth $B_{m,0}$ from the constraint $\tau_{c,0}^m \ge R_{c,0}$ as follows:

$$B_m \ge \frac{R_{c,0} N_{m,c}^{tol} \ln 2}{\exp\left\{\frac{W_0}{\rho_c}\right\} E_1\left(\frac{W_0}{\rho_c}\right)} \triangleq B_{m,0}. \tag{8}$$

Then, for problem (1), we have the following inequality from the constraint $\tau_{c,0} \ge R_{c,0}$:

$$N_{m,c} \le \frac{\exp\left\{\frac{W_0}{\rho_c}\right\} E_1\left(\frac{W_0}{\rho_c}\right)}{R_{c,0} \ln 2} \cdot B_m \triangleq H \cdot B_m. \tag{9}$$

Hence, the solution of problem (1) can be formulated as:

$$N_{m,c}^{\max} = H \cdot B_m, \quad B_m \le B_{m,0}. \qquad \blacksquare$$

After getting $B_{m,0}$ and $N_{m,c}^{\max} = H \cdot B_m$ from (8) and (9), the payoff of MNO m for scarce spectral bandwidth is:

$$U_m(B_m) = P_c \cdot H \cdot B_m - \frac{P}{2}\cdot B_m^2, \quad B_m \le B_{m,0}.$$

Obviously, the unconstrained optimal solution is $B_m^* = \frac{P_c H}{P}$. When $\frac{P_c H}{P} > B_{m,0}$, all cellular users can be served. In this case, MNOs can use MPMS-2 to decide the spectral bandwidth requirements. Thus, in MPMS-1, we only consider the case of $\frac{P_c H}{P} \le B_{m,0}$, and the corresponding optimal solution of MPMS-1 is:

$$U_{1,m}^* = \frac{(P_c H)^2}{2P}, \quad \frac{P_c H}{P} \le B_{m,0}, \tag{10}$$

$$(N_{m,c}^*, B_{1,m}^*) = (\frac{P_c H^2}{P}, \frac{P_c H}{P}), \quad \frac{P_c H}{P} \le B_{m,0}. \tag{11}$$

B. Optimal Solution for MPMS-2 of MNOs

Now, we turn to analyze the optimal solution of MPMS-2.

Lemma 2: The MNOs payoff maximization sub-game for the case of sufficient spectral bandwidth (i.e., MPMS-2) can be solved with linear complexity $\mathcal{O}(N_{m,I}^{tol})$.

Proof: Since $N_{m,I}^{\max}(B_m)$ in (7) (i.e., the maximum coexisting number of IoT devices for a given spectral bandwidth B_m) can be derived from problem (2), MPMS-2 in (7) can be transformed into the following equivalent problem:

$$\begin{aligned} \max_{N_{m,I}, B_m} \; & U_{2,m} = P_c \cdot N_{m,c}^{tol} + P_I \cdot N_{m,I} - \frac{P}{2}\cdot B_m^2 \\ \text{s.t.} \quad & B_m > B_{m,0}, \quad 0 < N_{m,I} \le N_{m,I}^{tol}, \\ & \tau_c^m \ge R_{c,0}, \quad \tau_r^m \ge R_{I,0}, \quad N_{m,I} \in \mathbb{N}. \end{aligned} \tag{12}$$

When constraints $N_{m,I} > 0$ and $\tau_c^m \ge R_{c,0}$ are satisfied, all the cellular users in MNO m can access. Then, the constraint $B_m > B_{m,0}$ is naturally satisfied and thus can be omitted.

In the following, to solve problem (12), we will first solve the optimal B_m as $B_{2,m}^*(N_{m,I})$ for a given $N_{m,I}$ and then determine the optimal $N_{m,I}^*$.

From *Proposition 2*, the average transmission rate of a cellular user coexisting with IoT devices is:

$$\tau_c^m = \frac{B_m}{N_{m,c}^{tol}} \frac{1}{\ln 2} \int_0^\infty \frac{1}{v+1} e^{-\frac{W_0}{\rho_c} v} \left(\frac{\rho_c}{v\rho_r + \rho_c} \right)^{N_{m,I} p_m p_l} dv.$$

Meanwhile, from *Proposition 3*, the average transmission rate of an IoT device coexisting with cellular users is:

$$\begin{aligned} \tau_r^m &= B_{m,r} \bar{\tau}_r^m \\ &= \frac{k p_m B_m}{F \cdot \ln 2} \int_0^\infty e^{-\frac{v W_0}{\rho_r}} \frac{\rho_r}{v\rho_c + \rho_r} \left(\frac{1}{v+1} \right)^{N_{m,I} p_m p_l} dv. \end{aligned}$$

Denote function $G(N_{m,I})$ as follows:

$$G(N_{m,I}) \triangleq \frac{R_{c,0} N_{m,c}^{tol} \ln 2}{\int_0^\infty \frac{1}{v+1} e^{-\frac{W_0}{\rho_c} v} \left(\frac{\rho_c}{v\rho_r + \rho_c} \right)^{N_{m,I} p_m p_l} dv}. \quad (13)$$

Then, we can deduce $B_m \geq G(N_{m,I})$ from the constraint $\tau_c^m(N_{m,I}, B_m) \geq R_{c,0}$ in (12). Similarly, denote function $K(N_{m,I})$ as follows:

$$K(N_{m,I}) \triangleq \frac{R_{I,0} F \ln 2}{k p_m \int_0^\infty e^{-\frac{v W_0}{\rho_r}} \frac{\rho_r}{v\rho_c + \rho_r} \left(\frac{1}{v+1} \right)^{N_{m,I} p_m p_l} dv}. \quad (14)$$

Thus, we have $B_m \geq K(N_{m,I})$ from the constraint $\tau_r^m(N_{m,I}, B_m) \geq R_{I,0}$ in (12). We can see that $G(N_{m,I})$ and $K(N_{m,I})$ are both strictly monotonically increasing with respect to $N_{m,I}$.

Then, the constraints $\tau_c^m(N_{m,I}, B_m) \geq R_{c,0}$ and $\tau_r^m(N_{m,I}, B_m) \geq R_{I,0}$ can be transformed into $B_m \geq \max\{G(N_{m,I}), K(N_{m,I})\}$. Meanwhile, because the objective function in problem (12) decreases with respect to B_m for fixed $N_{m,I}$, the optimal B_m is:

$$B_{2,m}^*(N_{m,I}) \triangleq \max\{G(N_{m,I}), K(N_{m,I})\}. \quad (15)$$

Therefore, problem (12) can be equivalently reformulated as

$$\begin{aligned} \max_{N_{m,I}} \quad & P_I \cdot N_{m,I} - \frac{P}{2} \cdot \left(B_{2,m}^*(N_{m,I}) \right)^2 \\ \text{s.t.} \quad & 0 < N_{m,I} \leq N_{m,I}^{tol}, \quad N_{m,I} \in \mathbb{N}. \end{aligned} \quad (16)$$

Notice that $N_{m,I}$ is the one-dimensional integer. When $N_{m,I}^*$ is determined, $B_{2,m}^*(N_{m,I}^*)$ is the optimal solution with an analytical form (15). Hence, we can apply the exhaustive method to obtain the optimal solution $(N_{m,I}^*, B_{2,m}^*)$ of problem (16) with linear complexity $\mathcal{O}(N_{m,I}^{tol})$. ■

After using Eqs. (10) and (15) to obtain the optimal solutions $B_{1,m}^*$ and $B_{2,m}^*$ of problems MPMS-1 and MPMS-2, respectively, we can derive the optimal spectral bandwidth strategy of MNO m as $\{U_m^*, B_m^*\}$ in MPMS, where $U_m^* = \max\{U_{1,m}^*, U_{2,m}^*\}$,

$$B_m^* = \begin{cases} B_{1,m}^*, & \text{if } U_{1,m}^* \geq U_{2,m}^*, \\ B_{2,m}^*, & \text{if } U_{1,m}^* < U_{2,m}^*. \end{cases} \quad (17)$$

It is worth noting that B_m^* is a function of price P.

C. Optimal Solution for WPMS of WSP

The WSP is assumed to offer a unit bandwidth price P based on the optimal solution B_m^* in (17) for MPMS of MNOs. Substituting (17) into WPMS (4), we can rewrite it as:

$$\begin{aligned} \max_P \quad & U_w(P) = \frac{P}{2} \cdot \left(\min\{ \sum_{m=1}^M B_m^*(P), B^{tol} \} \right)^2 - C \\ \text{s.t.} \quad & P \geq 0. \end{aligned} \quad (18)$$

It is easy to see that $B_m^*(P)$ is monotonically decreasing with respect to P. Thus, we propose an iterative pricing algorithm (IPA) to solve the WPMS (18). The core idea of IPA is gradually increasing price P to increase the WSP's payoff while ensuring that MNOs can use up the total marketable spectral bandwidth B^{tol}. Therefore, the increment in each iteration is proportional to the difference between the required spectral bandwidth of MNOs $\sum_{m=1}^M B_m^*(P)$ and the total marketable bandwidth B^{tol}. As a result, the iteration of unit bandwidth price P is carried out by the WSP as follows:

$$P_n = P_{n-1} + \alpha_n \cdot \left(\sum_{m=1}^M B_m^*(P_{n-1}) - B^{tol} \right), \quad (19)$$

where n is the iteration number and α_n is the price adjustment parameter. In order to avoid the case where the updated P oscillates around the optimal price, we can reduce the parameter α_n gradually to guarantee the convergence.

It should be noted that the operating mechanism of the multi-operator spectrum sharing architecture is as follows. When the bandwidth requirement of end users varies, MNOs and WSP will re-sign a spectrum sharing agreement, i.e., conduct Algorithm 1 to determine an equilibrium price and bandwidth allocation plans based on the current load conditions in the area. At the beginning of Algorithm 1, MNOs first observe their current loads, i.e., the numbers of cellular users and IoT devices that send the communication requests. In the iterative process of Algorithm 1, the WSP and MNOs only pass instructions between each other, which include the proposed bandwidth price of WSP and bandwidth purchase plans of MNOs. Only after an equilibrium price and bandwidth allocation plans are determined, i.e., the sharing agreement is achieved, the wireless spectrum resources will be authorized to the corresponding MNOs at the bandwidth price obtained.

D. Stackelberg Equilibrium and Optimality of the Algorithm

Definition3 (Stackelberg Equilibrium): The strategy profile $\{P^*, B_m^*\}$ is a Stackelberg equilibrium (SE) if for the WSP and each MNO $m \in M$, P^* and B_m^* are optimal control strategies when others' strategies are given.

We can see that, in this model, the SE is also a Nash equilibrium, where no one would benefit through making a unilateral change of strategy. To achieve the SE, a backward induction method is utilized to analyze the proposed game, which captures the cyclic dependency between MNOs and the WSP. We first provide some properties for the optimal solution of MPMS, and then show the condition that the optimal solution of WPMS should meet. Finally, based on the

Algorithm 1: Iterative Pricing Algorithm (IPA)

Input: P_1, P_c, P_I, $R_{c,0}$, $R_{I,0}$, B^{tol}, $N_{m,c}$, $N_{m,I}$, $m = 1, \cdots, M$, stopping tolerance ϵ.

Output: Spectral bandwidth price P^*, the optimal values of MNO payoff U_m and WSP payoff U_w.

for *iteration* $n = 1, 2, \cdots$ **do**
  for MNO $m = 1, \cdots, M$ **do**
    For spectral bandwidth price P_n, MNO solves MPMS-1 and MPMS-2 to get (17);
    Use (5) to calculate MNO payoff U_m;
  end
  The WSP uses (3) to calculate its payoff U_w;
  Update the spectral bandwidth price P_{n+1} using (19);
  if $|P_{n+1} - P_n| \leq \epsilon$ **then**
    No price change announcement to MNOs and an optimal Stakelberg equilibrium is reached. **STOP**;
  else
    Announce P_{n+1} to MNOs and go to Step 1;
  end
end

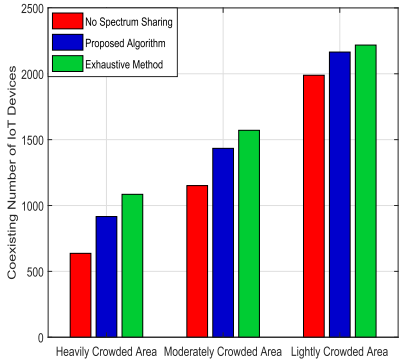

Fig. 3. Coexisting number of IoT devices versus bandwidth.

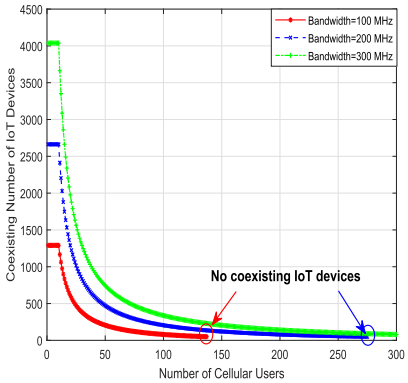

Fig. 4. Coexistence of cellular users and IoT devices at different bandwidths.

condition of the optimal solution of WPMS, the proposed IPA is proven to converge to the SE.

Lemma 3: The optimal solution B_m^* of MPMS is strictly decreasing with respect to the bandwidth price P.

Proof: See Appendix D. ■

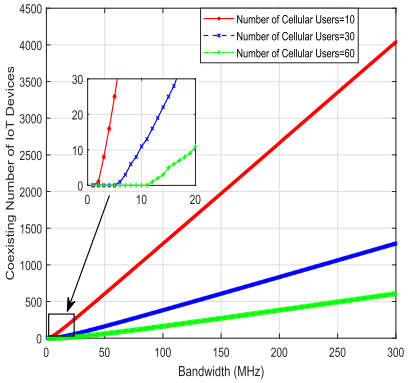

Fig. 5. Coexisting number of IoT devices versus bandwidth.

Before presenting the condition of the optimal solution of WPMS in problem (18), we first give some properties of functions $G(N_{m,I})$ and $K(N_{m,I})$ in MPMS-2.

Lemma 4: For the optimal solution $N_{m,I}^*$ of MPMS-2, $G(N_{m,I}^*)$ and $K(N_{m,I}^*)$ satisfy

$$\begin{cases} G'(N_{m,I}^*)^2 + G(N_{m,I}^*) \cdot G''(N_{m,I}^*) > 0, \\ K'(N_{m,I}^*)^2 + K(N_{m,I}^*) \cdot K''(N_{m,I}^*) > 0, \end{cases} \tag{20}$$

where G', K' and G'', K'' represent the first and second derivatives of function $G(\cdot)$ and function $K(\cdot)$ in (13) and (14), respectively.

Proof: See Appendix E. ■

The following theorem gives the condition of the optimal solution of WPMS in (18).

Theorem 1: Suppose that the price $\bar{P}$ satisfies the condition $\sum_{m=1}^{M} B_m^*(\bar{P}) = B^{tol}$ with $B_m^*(\bar{P})$ given by MPMS. Then, $\bar{P}$ is the optimal solution of WPMS.

Proof: See Appendix F. ■

According to *Lemma 3*, $B_m^*(P)$ is strictly decreasing with respect to price P. Combining with *Theorem 1*, we can gradually increase or decrease the bandwidth price P to reach the optimal condition $\sum_{m=1}^{M} B_m^*(\bar{P}) = B^{tol}$, which unveils the optimality of *Algorithm 1* to reach the SE.

VII. Numerical Analysis

Consider a multi-operator dynamic spectrum sharing scenario that supports the coexistence of cellular users and massive IoT devices under 3 MNOs and 1 WSP. Each MNO owns one BS in the local area. The cellular users and IoT devices access each MNO by obeying the coexisting access rules with the required rate $R_{c,0} = 1$ Mbps and $R_{I,0} = 0.1$ Mbps. The access prices of a cellular user and an IoT device are fixed as \$10 and \$1, respectively. In the simulation setup, we set the receive power threshold of cellular users and IoT devices to be $\rho_c = -70$ dBm and $\rho_r = -80$ dBm, respectively. The noise power $W_0 = -90$ dBm, path-loss exponents $\gamma_c = 3$, $\gamma_r = 4$, and the channel gain $h \sim \exp(1)$. The number of subchannels $F = 20$, and the maximum spectral bandwidth of WSP $B^{max} = 300$ MHz. Each IoT device randomly selects 4 subchannels as candidates (i.e., $k = 4$) and medium access probability is $p_m = 0.5$. For the WSP, the initial bandwidth

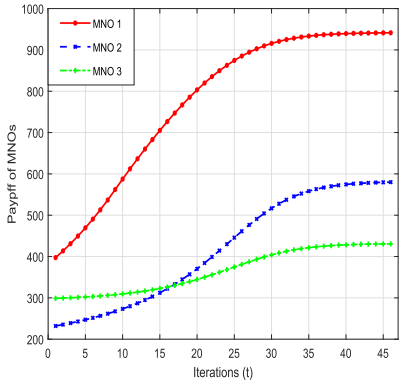

Fig. 6. Payoffs of three MNOs during the iterations of IPA in lightly CA.

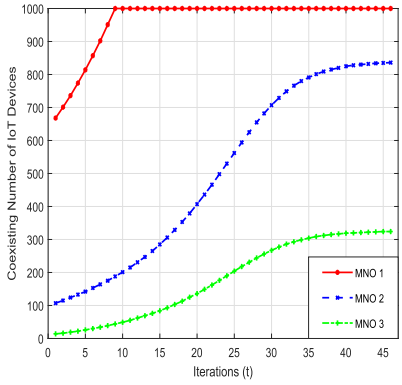

Fig. 7. Variation in the coexisting number of IoT devices for three MNOs in lightly CA.

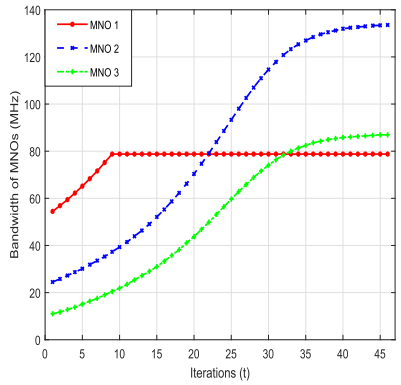

Fig. 8. Variation in the required bandwidths of three MNOs in lightly CA.

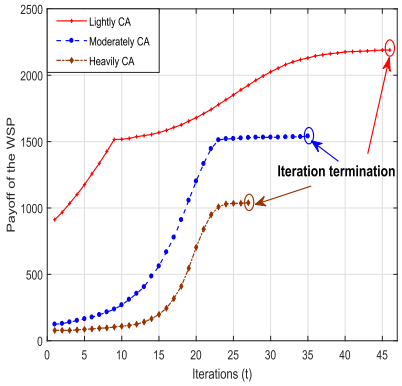

Fig. 9. Variation in the payoff of the WSP.

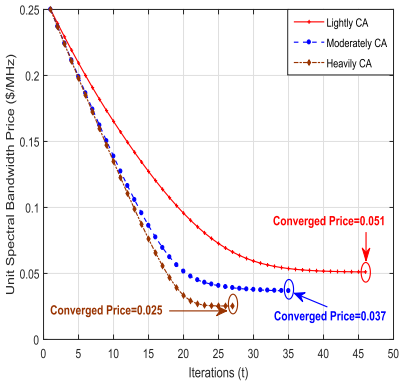

Fig. 10. Variation in the bandwidth price of the WSP.

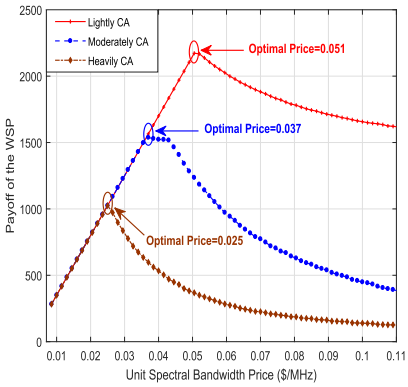

Fig. 11. The payoff of the WSP versus bandwidth price.

price is assumed to be \$0.25 per MHz, the spectrum fee paid to the FCC is $C = \$100$, and the price adjustment parameter is $\alpha_n = 0.00005$.

1) *Performance Comparison in Different Situations:* To evaluate the performance of the proposed algorithm under different situations, we simulate three different crowded areas (CAs), where the total numbers of cellular users in MNOs are $N_c^{tol} = \{10, 20, 30\}$ for lightly crowded area, $N_c^{tol} = \{20, 40, 60\}$ for moderately crowded area, and $N_c^{tol} = \{30, 60, 90\}$ for heavily crowded area. The total number of IoT devices is 1000 for all situations. Then, as shown in Fig. 3, we plot the coexisting number of IoT devices through the proposed algorithm, the no-sharing scheme, and the exhaustive method (i.e., globally optimal solution). The proposed algorithm can improve almost 50%, 30% and 10% in the three CAs compared with the no-sharing scheme. Also, there is less than about 10% gap between the proposed algorithm (i.e., Stackelberg equilibrium) and the exhaustive method (which is not applicable to real-time spectrum sharing scenarios).

2) *Performance Analysis of the Coexisting Access Rules:* We have plotted the maximum number of IoT devices that a BS can access under different spectral bandwidths, i.e., 100, 200 and 300 MHz. As shown in Fig. 4, the larger the spectral bandwidth is, the more IoT devices can access. Meanwhile,

when there are more cellular users, the fewer IoT devices can coexist. Similarly, we plot Fig. 5 to show the maximum number of IoT devices which can access the networks under different numbers of cellular users, i.e., $N_c^{tol} = \{10, 30, 60\}$. When the bandwidth is low, MNOs are preferred to satisfy cellular users. When the bandwidth is large, the number of IoT devices increases as the bandwidth increases. The more cellular users there are, the fewer number of coexisting IoT devices there will be.

3) *Performance of the MNOs:* In the following iteration, we display the situation of lightly crowded area to show the effectiveness and convergence of the proposed algorithm. First, the variation of expected payoffs of MNOs is shown in Fig. 6. It is easy to see that each MNO payoff is increasing until it converges. Next, we exhibit the variation of coexisting number of IoT devices versus iterations in Fig. 7. Finally, the variation of MNOs' required bandwidth versus iterations of IPA is plotted in Fig. 8. As the bandwidth price changes from high to low, MNOs purchase more and more bandwidths, which makes the coexisting number of IoT devices gradually increase until convergence.

4) *Performance of the WSP:* In Fig. 9, we plot the variation of expected payoff of the WSP. As the bandwidth price iterates, the WSP's payoff gradually increases to convergence. Next, the variation of bandwidth price versus the iterations is shown in Fig. 10. The price gradually decreases from a high initial price to the convergent solution. In order to verify the optimality of the proposed algorithm, Fig. 11 illustrates the payoff of WSP versus all the bandwidth prices. It can be seen that there is a unique optimal price, and the iterative algorithm can converge at the optimal Stackelberg equilibrium where each sub-game reaches its equilibrium that maximizes the payoffs of WSP and MNOs, respectively.

VIII. Conclusion and Future Work

In this paper, we have investigated a multi-operator spectrum sharing problem to support the coexistence of massive IoT devices and cellular users. Specifically, we have presented a Stackelberg pricing game framework to model and analyze the joint cyclic dynamic decision making problems among the WSP, MNOs, cellular users and IoT devices. The MNOs (i.e., followers) can maximize their payoffs by purchasing the optimal bandwidth to maximize the access number of cellular users and IoT devices, and the WSP (i.e., leader) maximizes its payoff by attracting more bandwidth requests from MNOs. The cellular users and IoT devices can access the networks and be served by the MNOs based on the proposed coexisting access rules. Based on the formulations, we have proposed an iterative algorithm for the Stackelberg pricing game, which can reach the equilibrium through iterating on WSP's bandwidth price. Furthermore, theoretical analysis and simulation results have proven that the proposed algorithm can converge to the Stackelberg equilibrium. In our future work, we will consider the spectrum multiplexing among MNOs and apply NOMA technologies to maximize the coexisting number of access IoT devices to further improve the spectrum utilization.

Appendix

A. Proof of Proposition 1

Utilizing stochastic geometry techniques, we first deduce the the complementary cumulative distribution function (CCDF) $p_c(\mathbf{x}, v)$ of the SNR of a cellular user as follows:

$$p_c(\mathbf{x}, v) = \mathbb{P}(\text{SNR}_c^l > v) = \mathbb{P}\left(h_c > \frac{vW_0}{\rho_c}\right) \overset{(i)}{=} \exp\left\{-\frac{vW_0}{\rho_c}\right\},$$

where (i) recalls that $h_c \sim \exp(1)$.

According to the Shannon's formula, we could calculate the average spectrum efficiency of transmission for the cellular users without IoT devices:

$$\begin{aligned}\bar{\tau}_{c,0} &= \mathbf{E}\left[\log_2(1+\text{SNR}_c^l)\right] = \int_0^\infty \mathbb{P}\left(\text{SNR}_c^l > 2^t - 1\right) dt \\ &= \int_0^\infty p_c(\mathbf{x}, 2^t-1)dt = \int_0^\infty \frac{1}{(v+1)\ln 2} p_c(\mathbf{x}, v)dv \\ &= \int_0^\infty \frac{1}{(v+1)\ln 2}\exp\left\{-\frac{vW_0}{\rho_c}\right\}dv \\ &= \frac{1}{\ln 2}\exp\left\{\frac{W_0}{\rho_c}\right\}E_1(\frac{W_0}{\rho_c}),\end{aligned}$$

where $E_1(x) = \int_x^\infty \frac{e^{-t}}{t}dt$ is the exponential integral.

B. Proof of Proposition 2

Using stochastic geometry, we first deduce the CCDF $p_c(\mathbf{x}, v)$ of the SINR for a cellular user coexisting with IoT devices as follows:

$$\begin{aligned}&p_c(\mathbf{x}, v) \\ &= \mathbb{P}(\text{SINR}_c^l > v) = \mathbb{P}\left(h_c > \frac{v}{\rho_c}(W_0 + I_c^l)\right) \\ &\overset{(i)}{=} \exp\left\{-\frac{v}{\rho_c}(W_0 + I_c^l)\right\} = \exp\left\{-\frac{vW_0}{\rho_c}\right\}\mathcal{L}_{I_c^l}\left(\frac{v}{\rho_c}\right),\end{aligned}$$

where I_c^l represents the interference from IoT devices on subchannel l, (i) comes from $h_c \sim \exp(1)$, and $\mathcal{L}_{I_c^l}(\cdot)$ denotes the Laplace transform of the interferences' probability density function. Define $s_c \triangleq v/\rho_c$ and let d_r be the distance between transfer and receiver. As we know $P_r d_r^{-\eta_r} = \rho_r$ from the truncated channel inversion power control scheme. Subsequently, it holds

$$\begin{aligned}\mathcal{L}_{I_c^l}(s_c) &= \mathbf{E}_{I_c^l}[e^{-s_c I_c^l}] = \mathbf{E}_{P_r,h_r,d_r}[e^{-s_c\sum_{X_i\in\Phi_r^l} P_r h_r d_r^{-\eta_r}}] \\ &\overset{(i)}{=} \prod_{X_i\in\Phi_r^l} \mathbf{E}_{h_r}[e^{-s_c\rho_r h_r}],\end{aligned}$$

where (i) follows from *Assumption 1*. Combining with

$$\mathbf{E}_{h_r}[e^{-s_c\rho_r h_r}] = \int_0^\infty e^{-s_c\rho_r x}\cdot e^{-x}dx = \frac{1}{s_c\rho_r + 1},$$

we can deduce

$$\mathcal{L}_{I_c^l}(s_c) = \prod_{X_i\in\Phi_r^l} \mathbf{E}_{h_r}[e^{-s_c\rho_r h_r}] = \left(\frac{1}{s_c\rho_r+1}\right)^{|\Phi_r^l|},$$

where $|\Phi_r^l| = N_I p_m p_l$ represents the number of IoT devices choosing subchannel l.

On the basis of the Shannon's formula, we could calculate the average spectrum efficiency of transmission for the cellular users coexisting with IoT devices:

$$\begin{aligned}\bar{\tau}_c &= \mathbf{E}\left[\log_2(1+\text{SINR}_c^l)\right] = \int_0^\infty \mathbb{P}\left(\text{SINR}_c^l > 2^t - 1\right) dt \\ &= \int_0^\infty p_c(\mathbf{x}, 2^t-1)dt = \int_0^\infty \frac{1}{(v+1)\ln 2} p_c(\mathbf{x}, v)dv \\ &= \int_0^\infty \frac{1}{(v+1)\ln 2} \exp\left\{-\frac{vW_0}{\rho_c}\right\} \mathcal{L}_{I_c^l}\left(\frac{v}{\rho_c}\right) dv \\ &= \frac{1}{\ln 2}\int_0^\infty \frac{1}{v+1} e^{-\frac{W_0}{\rho_c}v} \left(\frac{\rho_c}{v\rho_r+\rho_c}\right)^{N_I p_m p_l} dv.\end{aligned}$$

C. Proof of Proposition 3

The CCDF $p_r(\mathbf{x}, v)$ of the SINR for an IoT device coexisting with cellular users is:

$$\begin{aligned}p_r(\mathbf{x}, v) &= \mathbb{P}(\text{SINR}_r^l > v) = \mathbb{P}\left(h_r > \frac{v}{\rho_r}(W_0 + I_{cr}^l + I_{rr}^l)\right) \\ &\overset{(i)}{=} \exp\left\{-\frac{v}{\rho_r}(W_0 + I_{cr}^l + I_{rr}^l)\right\} \\ &= \exp\left\{-\frac{vW_0}{\rho_r}\right\} \mathcal{L}_{I_{cr}^l}\left(\frac{v}{\rho_r}\right) \mathcal{L}_{I_{rr}^l}\left(\frac{v}{\rho_r}\right),\end{aligned}$$

where I_{cr}^l and I_{rr}^l represent the interferences from the cellular user and IoT devices on subchannel l, respectively, (i) follows from $h_r \sim \exp(1)$. Denote $s_r \triangleq v/\rho_r$. Based on *Assumption 1*, we have

$$\begin{aligned}\mathcal{L}_{I_{cr}^l}(s_r) &= \mathbf{E}_{I_{cr}^l}[e^{-s_r I_{cr}^l}] = \mathbf{E}_{h_c}[e^{-s_r \rho_c h_c}] \\ &= \int_0^\infty e^{-s_r\rho_c x} \cdot e^{-x} dx = \frac{1}{s_r\rho_c + 1}.\end{aligned}$$

On the other hand, for $\mathcal{L}_{I_{rr}^l}(s_r)$, we have

$$\begin{aligned}\mathcal{L}_{I_{rr}^l}(s_r) &= \mathbf{E}_{I_{rr}^l}[e^{-s_r I_{rr}^l}] = \mathbf{E}_{h_r}[e^{-s_r \sum_{X_i\in\Phi_{rr}^l} \rho_r h_r}] \\ &= \prod_{X_i\in\Phi_{rr}^l} \mathbf{E}_{h_r}[e^{-s_r\rho_r h_r}] = \prod_{X_i\in\Phi_{rr}^l} \mathbf{E}_{h_r}[e^{-vh_r}],\end{aligned}$$

Subsequently, it follows

$$\mathbf{E}_{h_r}[e^{-vh_r}] = \int_0^\infty e^{-vx}\cdot e^{-x}dx = \frac{1}{v+1}.$$

Owing to the independence between IoT devices, we obtain

$$\mathcal{L}_{I_{rr}^l}(s_r) = \textstyle\prod_{X_i\in\Phi_{rr}^l} \mathbf{E}_{h_r}[e^{-s_r\rho_r h_r}] = \left(\frac{1}{v+1}\right)^{|\Phi_{rr}^l|},$$

where $|\Phi_{rr}^l| = N_I p_m p_l - 1$ represents the number of other interferers of IoT devices choosing subchannel l.

According to the Shannon's formula, we could derive the average spectrum efficiency of an IoT device when coexisting with cellular users as follows:

$$\begin{aligned}\bar{\tau}_r &= \mathbf{E}\left[\log_2(1+\text{SINR}_r^l)\right] = \int_0^\infty \mathbb{P}\left[\text{SINR}_r^l > 2^t - 1\right] dt \\ &= \int_0^\infty p_r(\mathbf{x}, 2^t-1)dt = \int_0^\infty \frac{1}{(v+1)\ln 2} p_r(\mathbf{x}, v)dv \\ &= \int_0^\infty \frac{1}{(v+1)\ln 2} e^{-\frac{W_0}{\rho_r}v} \mathcal{L}_{I_{cr}^l}\left(\frac{v}{\rho_r}\right) \mathcal{L}_{I_{rr}^l}\left(\frac{v}{\rho_r}\right) dv \\ &= \frac{1}{\ln 2}\int_0^\infty e^{-\frac{W_0}{\rho_r}v} \frac{\rho_r}{v\rho_c+\rho_r} \left(\frac{1}{v+1}\right)^{N_I p_m p_l} dv.\end{aligned}$$

D. Proof of Lemma 3

Recalling the optimal solution B_m^* of MPMS in (17), we can divide the monotonicity arguments of B_m^* into two cases, i.e., $B_m^* = B_{1,m}^*$ and $B_m^* = B_{2,m}^*$.

When $B_m^* = B_{1,m}^*$, the optimal solution of MPMS comes from MPMS-1, i.e., $B_m^* = \frac{P_c H}{P}$. We can conclude that B_m^* is strictly decreasing with respect to the bandwidth price P.

When $B_m^* = B_{2,m}^*$, the optimal solution results from MPMS-2. In order to prove its monotonicity, we assume that there are two pairs of optimal solutions $(\hat{N}_{m,I}^*, \hat{B}_m^*)$ and $(\check{N}_{m,I}^*, \check{B}_m^*)$ from MPMS-2 under different bandwidth prices $\hat{P}$ and $\check{P}$, respectively. Without loss of generality, we suppose that $\hat{P} > \check{P}$. According to the optimality of MPMS-2 in problem (16), we have:

$$\begin{aligned}P_I\hat{N}_{m,I}^* - \frac{\hat{P}}{2}(\hat{B}_m^*)^2 &> P_I\check{N}_{m,I}^* - \frac{\hat{P}}{2}(\check{B}_m^*)^2, \\ P_I\check{N}_{m,I}^* - \frac{\check{P}}{2}(\check{B}_m^*)^2 &> P_I\hat{N}_{m,I}^* - \frac{\check{P}}{2}(\hat{B}_m^*)^2.\end{aligned}$$

Then, by adding the above two inequalities and doing simple manipulations, we can derive that

$$\hat{P}\left[(\check{B}_m^*)^2 - (\hat{B}_m^*)^2\right] > \check{P}\left[(\check{B}_m^*)^2 - (\hat{B}_m^*)^2\right].$$

Recalling that $\hat{P} > \check{P} > 0$, $\hat{B}_m^* > 0$, and $\check{B}_m^* > 0$, the above inequality means $\check{B}_m^* > \hat{B}_m^*$, i.e., B_m^* is strictly decreasing with respect to price P. As $N_{m,I}^*$ is strictly increasing with respect to B_m^*, we can conclude that $N_{m,I}^*$ is also strictly decreasing with respect to price P.

E. Proof of Lemma 4

Define $N_{m,I}^*$ as the optimal solution of problem (16). We first analyze the property of $N_{m,I}^*$. For the notation brevity, let $U(N_{m,I}) \triangleq P_I \cdot N_{m,I} - \frac{P}{2}\cdot\left(B_m^*(N_{m,I})\right)^2$. According to the definition of $B_m^*(N_{m,I})$ in (15), its derivative is

$$\frac{\partial B_m^*(N_{m,I})}{\partial N_{m,I}} = \begin{cases} G'(N_{m,I}), & \text{Case 1} \\ K'(N_{m,I}), & \text{Case 2,}\end{cases}$$

where Case 1 and Case 2 correspond to $G(N_{m,I}) \geq K(N_{m,I})$ and $G(N_{m,I}) < K(N_{m,I})$, respectively. Then, the derivative of $U(N_{m,I})$ is given by

$$\begin{aligned}U'(N_{m,I}) &\triangleq \frac{\partial U(N_{m,I})}{\partial N_{m,I}} \\ &= \begin{cases} P_I - P\cdot G(N_{m,I})\cdot G'(N_{m,I}), & \text{Case 1} \\ P_I - P\cdot K(N_{m,I})\cdot K'(N_{m,I}), & \text{Case 2.}\end{cases}\end{aligned}$$

For problem (16), constraint $0 < N_{m,I} \leq N_{m,I}^{tol}$ is equal to $0 < N_{m,I} < N_{m,I}^{tol} + 1$ for $N_{m,I} \in \mathbb{N}$. In the following, because the objective function in (16) is continuous with respect to $N_{m,I}$, the integer constraint is reasonable to be ignored when analyzing the property of the optimal solution $N_{m,I}^*$. By introducing Lagrangian multipliers $\lambda_0 > 0$ and $\lambda_1 > 0$ for constraint $0 < N_{m,I} < N_{m,I}^{tol} + 1$, the corresponding Lagrangian function is $L(N_{m,I}, \lambda_0, \lambda_1) = U(N_{m,I}) + \lambda_0\ N_{m,I} + \lambda_1(N_{m,I}^{tol} + 1 - N_{m,I})$. Since the optimal solution $N_{m,I}^*$ is also a Karush-Kuhn-Tucker (KKT) point of problem (16), $N_{m,I}^*$ should satisfy the KKT condition [34]:

$$\frac{\partial L(N_{m,I}^*, \lambda_0, \lambda_1)}{\partial N_{m,I}} = U'(N_{m,I}^*) + \lambda_0 - \lambda_1 = 0,$$

together with the complementary slackness conditions $\lambda_0\ N_{m,I}^* = 0$ and $\lambda_1(N_{m,I}^{tol} + 1 - N_{m,I}^*) = 0$. Due to $0 < N_{m,I}^* < N_{m,I}^{tol} + 1$, we have $\lambda_0 = \lambda_1 = 0$. As a consequence, it holds $U'(N_{m,I}^*) = 0$. Because

$$\begin{aligned} &U''(N_{m,I}) \\ &\triangleq \frac{\partial U'(N_{m,I})}{\partial N_{m,I}} \\ &= \begin{cases} -P\left(G'(N_{m,I})^2 + G(N_{m,I}) \cdot G''(N_{m,I})\right), & \text{Case 1} \\ -P\left(K'(N_{m,I})^2 + K(N_{m,I}) \cdot K''(N_{m,I})\right), & \text{Case 2,} \end{cases} \end{aligned}$$

and $U''(N_{m,I}) \neq 0$, $U'(N_{m,I}^*) = 0$ defines $N_{m,I}^*$ as an implicit function of P. According to the implicit function theorem (Theorem 5.14 in [35]), $N_{m,I}^*$ is differentiable with respect to P and

$$\begin{aligned} &N'_{m,I} \\ &\triangleq \frac{\partial N_{m,I}^*}{\partial P} = -\left(\frac{\partial U'(N_{m,I}^*)}{\partial P}\right) / U''(N_{m,I}^*) \\ &= \begin{cases} -\dfrac{G(N_{m,I}^*)G'(N_{m,I}^*)}{P\left(G'(N_{m,I}^*)^2 + G(N_{m,I}^*) \cdot G''(N_{m,I}^*)\right)}, & \text{Case 1} \\ -\dfrac{K(N_{m,I}^*)K'(N_{m,I}^*)}{P\left(K'(N_{m,I}^*)^2 + K(N_{m,I}^*) \cdot K''(N_{m,I}^*)\right)}, & \text{Case 2.} \end{cases} \end{aligned}$$

Invoking the definitions of $G(N_{m,I})$ and $K(N_{m,I})$ in (13) and (14), we can get $G(N_{m,I}^*) > 0$, $G'(N_{m,I}^*) > 0$, $K(N_{m,I}^*) > 0$ and $K'(N_{m,I}^*) > 0$. Meanwhile, on the basis of *Lemma 3*, $N_{m,I}^*$ is strictly decreasing with respect to P, i.e., $N'_{m,I} < 0$. Hence, (20) holds true.

F. Proof of Theorem 1

We first analyze the monotonicity of $U_w(P)$, which are divided into two situations.

Situation 1: $P \leq \bar{P}$.

According to definition of $\bar{P}$, i.e., $\sum_{m=1}^{M} B_m^*(\bar{P}) = B^{tol}$, and the fact that $B_m^*(P)$ is decreasing with respect to P for each $m \in M$ by *Lemma 3*, then we can derive $\sum_{m=1}^{M} B_m^*(P) \geq B^{tol}$. In this case, $U_w(P) = \frac{P}{2}(B^{tol})^2 - C$, which is obviously increasing with respect to P.

Situation 2: $P > \bar{P}$.

In this case, we have $\sum_{m=1}^{M} B_m^*(P) < B^{tol}$, which leads to $U_w(P) = \frac{P}{2}\left(\sum_{m=1}^{M} B_m^*(P)\right)^2 - C$. Then, the derivative of $U_w(P)$ with respect to P is

$$U'_w(P) \triangleq \frac{\partial U_w(P)}{\partial P} = \frac{1}{2}\left(\sum_{m=1}^{M} B_m^*(P)\right)\left(\sum_{m=1}^{M} \Lambda_m\right), \quad (21)$$

where $\Lambda_m \triangleq B_m^*(P) + 2P\frac{\partial B_m^*(P)}{\partial P}$. In the following, we will prove $\Lambda_m < 0$, $\forall m \in M$.

Recalling the optimal solution of MNOs in (17), if $B_m^*(P)$ comes from MPMS-1, i.e., $B_m^*(P) = B_{1,m}^*(P)$, it follows from (11) that $B_m^*(P) = \frac{P_c H}{P}$. Then, it is easy to deduce $\Lambda_m = -\frac{P_c H}{P} < 0$.

If $B_m^*(P)$ comes from MPMS-2, i.e., $B_m^*(P) = B_{2,m}^*(N_{m,I}^*(P))$ with $B_{2,m}^*(N_{m,I}^*(P))$ given in (15), according to the chain rule [36], we can obtain Λ_m as follows:

$$\Lambda_m = B_m^*(N_{m,I}^*(P)) + 2P\frac{\partial B_m^*(N_{m,I}^*(P))}{\partial N_{m,I}} N'_{m,I}.$$

Plugging $B_m^*(N_{m,I})$ in (15) and expressions of $\frac{\partial B_m^*(N_{m,I})}{\partial N_{m,I}}$ and $N'_{m,I}$ in Appendix E, we can obtain

$$\begin{aligned} &\Lambda_m \\ &= \begin{cases} \dfrac{G(N_{m,I}^*)[G(N_{m,I}^*)G''(N_{m,I}^*) - G'(N_{m,I}^*)^2]}{G'(N_{m,I}^*)^2 + G(N_{m,I}^*)G''(N_{m,I}^*)}, & \text{Case 3} \\ \dfrac{K(N_{m,I}^*)[K(N_{m,I}^*)K''(N_{m,I}^*) - K'(N_{m,I}^*)^2]}{K'(N_{m,I}^*)^2 + K(N_{m,I}^*)K''(N_{m,I}^*)}, & \text{Case 4,} \end{cases} \end{aligned}$$

where Case 3 and Case 4 represent $G(N_{m,I}^*) \geq K(N_{m,I}^*)$ and $G(N_{m,I}^*) < K(N_{m,I}^*)$, respectively.

Recalling the definition of $G(N_{m,I})$ in (13) and using the Leibniz integral rule [37] to exchange the order of integral and derivative, we can deduce

$$\begin{aligned} &G'(N_{m,I}^*) \\ &= -R_{c,0} N_{m,c} \ln 2 \\ &\quad \times \frac{\int_0^\infty \frac{\ln\left(\frac{\rho_c}{v\rho_r + \rho_c}\right)}{v+1} e^{-\frac{W_0}{\rho_c} v} \left(\frac{\rho_c}{v\rho_r + \rho_c}\right)^{N_{m,I} p_m p_l} dv}{\left(\int_0^\infty \frac{1}{v+1} e^{-\frac{W_0}{\rho_c} v} \left(\frac{\rho_c}{v\rho_r + \rho_c}\right)^{N_{m,I} p_m p_l} dv\right)^2}, \\ &G''(N_{m,I}^*) \\ &= 2R_{c,0} N_{m,c} \ln 2 \\ &\quad \times \frac{\left(\int_0^\infty \frac{\ln\left(\frac{\rho_c}{v\rho_r + \rho_c}\right)}{v+1} e^{-\frac{W_0}{\rho_c} v} \left(\frac{\rho_c}{v\rho_r + \rho_c}\right)^{N_{m,I} p_m p_l} dv\right)^2}{\left(\int_0^\infty \frac{1}{v+1} e^{-\frac{W_0}{\rho_c} v} \left(\frac{\rho_c}{v\rho_r + \rho_c}\right)^{N_{m,I} p_m p_l} dv\right)^3} \\ &\quad - R_{c,0} \\ &\quad \times \frac{N_{m,c} \ln 2 \int_0^\infty \frac{\ln^2\left(\frac{\rho_c}{v\rho_r + \rho_c}\right)}{v+1} e^{-\frac{W_0}{\rho_c} v} \left(\frac{\rho_c}{v\rho_r + \rho_c}\right)^{N_{m,I} p_m p_l} dv}{\left(\int_0^\infty \frac{1}{v+1} e^{-\frac{W_0}{\rho_c} v} \left(\frac{\rho_c}{v\rho_r + \rho_c}\right)^{N_{m,I} p_m p_l} dv\right)^2}. \end{aligned}$$

Hence, we further have

$$G(N^*_{m,I})G''(N^*_{m,I}) - G'(N^*_{m,I})^2 = \frac{(R_{c,0}N_{m,c}\ln 2)^2}{\left(\int_0^\infty \frac{1}{v+1}e^{-\frac{W_0}{\rho_c}v}\left(\frac{\rho_c}{v\rho_r+\rho_c}\right)^{N_{m,I}p_m p_l} dv\right)^4} \times \left[\left(\int_0^\infty \frac{\ln\left(\frac{\rho_c}{v\rho_r+\rho_c}\right)}{v+1}e^{-\frac{W_0}{\rho_c}v}\left(\frac{\rho_c}{v\rho_r+\rho_c}\right)^{N_{m,I}p_m p_l} dv\right)^2 - \int_0^\infty \frac{\ln^2\left(\frac{\rho_c}{v\rho_r+\rho_c}\right)}{v+1}e^{-\frac{W_0}{\rho_c}v}\left(\frac{\rho_c}{v\rho_r+\rho_c}\right)^{N_{m,I}p_m p_l} dv \times \int_0^\infty \frac{1}{v+1}e^{-\frac{W_0}{\rho_c}v}\left(\frac{\rho_c}{v\rho_r+\rho_c}\right)^{N_{m,I}p_m p_l} dv\right].$$

Based on the well-known Cauchy-Schwarz equality, i.e., $(\int f(v)g(v)dv)^2 \le (\int |f(v)|^2\, dv)(\int |g(v)|^2\, dv)$, it immediately yields $G(N^*_{m,I})G''(N^*_{m,I}) - G'(N^*_{m,I})^2 \le 0$ by substituting $|f(v)|^2$ by $\frac{\ln^2\left(\frac{\rho_c}{v\rho_r+\rho_c}\right)}{v+1}e^{-\frac{W_0}{\rho_c}v}\left(\frac{\rho_c}{v\rho_r+\rho_c}\right)^{N_{m,I}p_m p_l}$ and $|g(v)|^2$ by $\frac{1}{v+1}e^{-\frac{W_0}{\rho_c}v}\left(\frac{\rho_c}{v\rho_r+\rho_c}\right)^{N_{m,I}p_m p_l}$. Observing that $f(v)$ and $g(v)$ are not linearly dependent, we have $G(N^*_{m,I})G''(N^*_{m,I}) - G'(N^*_{m,I})^2 < 0$. Combined with *Lemma 4*, i.e., $G'(N^*_{m,I})^2 + G(N^*_{m,I})G''(N^*_{m,I}) > 0$ in (20), we conclude $\Lambda_m < 0$ for Case 3. Following the similar arguments, we also have $\Lambda_m < 0$ for Case 4. Consequently, equality (21) implies $U'_w(P) < 0$. Therefore, when $P > \bar{P}$, $U_w(P)$ is decreasing with respect to the bandwidth price P.

On the basis of the above arguments of **Situation 1** and **Situation 2**, we can conclude that $U_w(P)$ should reach its maximum at $\bar{P}$ satisfying $\sum_{m=1}^{M} B^*_m(N^*_{m,I}(\bar{P})) = B^{tol}$.

REFERENCES

[1] Y. Meng, W. Zhang, H. Zhu, and X. S. Shen, "Securing consumer IoT in the smart home: Architecture, challenges, and countermeasures," *IEEE Wireless Commun.*, vol. 25, no. 6, pp. 53–59, Dec. 2018.

[2] Q. Yuan, H. Zhou, Z. Liu, J. Li, F. Yang, and X. Shen, "CESense: Cost-effective urban environment sensing in vehicular sensor networks," *IEEE Trans. Intell. Transp. Syst.*, vol. 20, no. 9, pp. 3235–3246, Sep. 2019.

[3] S. Verma, Y. Kawamoto, Z. M. Fadlullah, H. Nishiyama, and N. Kato, "A survey on network methodologies for real-time analytics of massive IoT data and open research issues," *IEEE Commun. Surveys Tuts.*, vol. 19, no. 3, pp. 1457–1477, 3rd Quart., 2017.

[4] B. Qian, H. Zhou, F. Lyu, J. Li, T. Ma, and F. Hou, "Toward collision-free and efficient coordination for automated vehicles at unsignalized intersection," *IEEE Internet Things J.*, vol. 6, no. 6, pp. 10408–10420, Dec. 2019.

[5] H. Zhou, N. Cheng, J. Wang, J. Chen, Q. Yu, and X. Shen, "Toward dynamic link utilization for efficient vehicular edge content distribution," *IEEE Trans. Veh. Technol.*, vol. 68, no. 9, pp. 8301–8313, Sep. 2019.

[6] 5G Americas White Papers. (Jul. 2019). *5G: The Future of IoT*. [Online]. Available: https://www.5gamericas.org/5g-the-future-of-iot/

[7] R. Jia, X. Chen, Q. Qi, and H. Lin, "Massive beam-division multiple access for B5G cellular Internet of Things," *IEEE Internet Things J.*, vol. 7, no. 3, pp. 2386–2396, Mar. 2020.

[8] X. Shao, X. Chen, C. Zhong, J. Zhao, and Z. Zhang, "A unified design of massive access for cellular Internet of Things," *IEEE Internet Things J.*, vol. 6, no. 2, pp. 3934–3947, Apr. 2019.

[9] K. Samdanis, X. Costa-Perez, and V. Sciancalepore, "From network sharing to multi-tenancy: The 5G network slice broker," *IEEE Commun. Mag.*, vol. 54, no. 7, pp. 32–39, Jul. 2016.

[10] *Telecommunication Management; Network Sharing; Concepts and Requirements*, document 3GPP, TS 32.130, Jun. 2016.

[11] R. H. Tehrani, S. Vahid, D. Triantafyllopoulou, H. Lee, and K. Moessner, "Licensed spectrum sharing schemes for mobile operators: A survey and outlook," *IEEE Commun. Surveys Tuts.*, vol. 18, no. 4, pp. 2591–2623, 4th Quart., 2016.

[12] L. Zhang, Y.-C. Liang, and M. Xiao, "Spectrum sharing for Internet of Things: A survey," *IEEE Wireless Commun.*, vol. 26, no. 3, pp. 132–139, Jun. 2019.

[13] Q. Yu, J. Ren, Y. Fu, Y. Li, and W. Zhang, "Cybertwin: An origin of next generation network architecture," *IEEE Wireless Commun.*, vol. 26, no. 6, pp. 111–117, Dec. 2019.

[14] N. Jiang, Y. Deng, A. Nallanathan, X. Kang, and T. Q. S. Quek, "Analyzing random access collisions in massive IoT networks," *IEEE Trans. Wireless Commun.*, vol. 17, no. 10, pp. 6853–6870, Oct. 2018.

[15] M. Gharbieh, H. ElSawy, A. Bader, and M.-S. Alouini, "Spatiotemporal stochastic modeling of IoT enabled cellular networks: Scalability and stability analysis," *IEEE Trans. Commun.*, vol. 65, no. 8, pp. 3585–3600, Aug. 2017.

[16] C. Liang and F. R. Yu, "Wireless network virtualization: A survey, some research issues and challenges," *IEEE Commun. Surveys Tuts.*, vol. 17, no. 1, pp. 358–380, 1st Quart., 2015.

[17] X. Costa-Perez, J. Swetina, T. Guo, R. Mahindra, and S. Rangarajan, "Radio access network virtualization for future mobile carrier networks," *IEEE Commun. Mag.*, vol. 51, no. 7, pp. 27–35, Jul. 2013.

[18] D. B. Rawat, A. Alshaikhi, A. Alshammari, C. Bajracharya, and M. Song, "Payoff optimization through wireless network virtualization for IoT applications: A three layer game approach," *IEEE Internet Things J.*, vol. 6, no. 2, pp. 2797–2805, Apr. 2019.

[19] N. N. Sapavath and D. B. Rawat, "Wireless virtualization architecture: Wireless networking for Internet of Things," *IEEE Internet Things J.*, vol. 7, no. 7, pp. 5946–5953, Jul. 2020.

[20] M. Shirvanimoghaddam, M. Dohler, and S. J. Johnson, "Massive non-orthogonal multiple access for cellular IoT: Potentials and limitations," *IEEE Commun. Mag.*, vol. 55, no. 9, pp. 55–61, Sep. 2017.

[21] H. Zhou, N. Cheng, Q. Yu, X. Sherman Shen, D. Shan, and F. Bai, "Toward multi-radio vehicular data piping for dynamic DSRC/TVWS spectrum sharing," *IEEE J. Sel. Areas Commun.*, vol. 34, no. 10, pp. 2575–2588, Oct. 2016.

[22] P. Semasinghe, S. Maghsudi, and E. Hossain, "Game theoretic mechanisms for resource management in massive wireless IoT systems," *IEEE Commun. Mag.*, vol. 55, no. 2, pp. 121–127, Feb. 2017.

[23] Q. Yu *et al.*, "A fully-decoupled RAN architecture for 6G inspired by neurotransmission," *J. Commun. Inf. Netw.*, vol. 4, no. 4, pp. 15–23, Dec. 2019.

[24] Y. Xiao, D. Niyato, Z. Han, and K.-C. Chen, "Secondary users entering the pool: A joint optimization framework for spectrum pooling," *IEEE J. Sel. Areas Commun.*, vol. 32, no. 3, pp. 572–588, Mar. 2014.

[25] Y. Xiao, M. Krunz, and T. Shu, "Multi-operator network sharing for massive IoT," *IEEE Commun. Mag.*, vol. 57, no. 4, pp. 96–101, Apr. 2019.

[26] D. Zhai, R. Zhang, L. Cai, and F. R. Yu, "Delay minimization for massive Internet of Things with non-orthogonal multiple access," *IEEE J. Sel. Topics Signal Process.*, vol. 13, no. 3, pp. 553–566, Jun. 2019.

[27] H. G. Moussa and W. Zhuang, "Energy- and delay-aware two-hop NOMA-enabled massive cellular IoT communications," *IEEE Internet Things J.*, vol. 7, no. 1, pp. 558–569, Jan. 2020.

[28] B. Singh *et al.*, "Coordination protocol for inter-operator spectrum sharing in co-primary 5G small cell networks," *IEEE Commun. Mag.*, vol. 53, no. 7, pp. 34–40, Jul. 2015.

[29] Y. Gu, Q. Cui, Q. Ye, and W. Zhuang, "Game-theoretic optimization for machine-type communications under QoS guarantee," *IEEE Internet Things J.*, vol. 6, no. 1, pp. 790–800, Feb. 2019.

[30] H. ElSawy, E. Hossain, and M.-S. Alouini, "Analytical modeling of mode selection and power control for underlay D2D communication in cellular networks," *IEEE Trans. Commun.*, vol. 62, no. 11, pp. 4147–4161, Nov. 2014.

[31] N. Cheng *et al.*, "Performance analysis of vehicular device-to-device underlay communication," *IEEE Trans. Veh. Technol.*, vol. 66, no. 6, pp. 5409–5421, Jun. 2017.

[32] H. G. Moussa and W. Zhuang, "RACH performance analysis for large-scale cellular IoT applications," *IEEE Internet Things J.*, vol. 6, no. 2, pp. 3364–3372, Apr. 2019.

[33] K. Zhu and E. Hossain, "Joint mode selection and spectrum partitioning for device-to-device communication: A dynamic stackelberg game," *IEEE Trans. Wireless Commun.*, vol. 14, no. 3, pp. 1406–1420, Mar. 2015.

[34] S. Boyd and L. Vandenberghe, *Convex Optimization*. Cambridge, U.K.: Cambridge Univ. Press, 2004.
[35] J. F. Bonnans and A. Shapiro, *Perturbation Analysis of Optimization Problems*. Cham, Switzerland: Springer, 2013.
[36] H.-N. Huang, S. A. M. Marcantognini, and N. J. Young, "Chain rules for higher derivatives," *Math. Intelligencer*, vol. 28, no. 2, pp. 61–69, Mar. 2006.
[37] H. Flanders, "Differentiation under the integral sign," *Amer. Math. Monthly*, vol. 80, no. 6, pp. 615–627, Jun. 1973.

Bo Qian (Student Member, IEEE) received the B.S. and M.S. degrees in statistics from Sichuan University, Chengdu, China, in 2015 and 2018, respectively. He is currently pursuing the Ph.D. degree with the School of Electronic Science and Engineering, Nanjing University, China. His current research interests include intelligent transportation systems and vehicular networks, wireless resource management, blockchain, convex optimization theory, and game theory.

Haibo Zhou (Senior Member, IEEE) received the Ph.D. degree in information and communication engineering from Shanghai Jiao Tong University, Shanghai, China, in 2014. From 2014 to 2017, he was a Post-Doctoral Fellow with Broadband Communications Research Group, Department of Electrical and Computer Engineering, University of Waterloo. He is currently an Associate Professor with the School of Electronic Science and Engineering, Nanjing University, Nanjing, China. His research interests include resource management and protocol design in vehicular ad hoc networks, cognitive networks, and space-air-ground integrated networks. He was a recipient of the 2019 IEEE ComSoc Asia-Pacific Outstanding Young Researcher Award. He has served as the Invited Track Co-Chair for ICCC'2019 and VTC-Fall'2020 and a TPC Member of many IEEE conferences, including GLOBECOM, ICC, and VTC. He has served as an Associate Editor for the IEEE Comsoc Technically Co-Sponsored the *Journal of Communications and Information Networks* (JCIN) from April 2017 to March 2019, and a Guest Editor for the *IEEE Communications Magazine* in 2016, the Hindawi *International Journal of Distributed Sensor Networks* in 2017, and *IET Communications* in 2017. He is currently an Associate Editor of the IEEE INTERNET OF THINGS JOURNAL, the *IEEE Network Magazine*, and the IEEE WIRELESS COMMUNICATIONS LETTER.

Ting Ma (Student Member, IEEE) received the B.S., M.S., and Ph.D. degrees in statistics from Sichuan University, Chengdu, China, in 2013, 2016, and 2020, respectively. She is currently a Post-Doctoral with the School of Electronic Science and Engineering, Nanjing University, Nanjing, China. Her current research interests mainly include robust hypothesis testing, space-air-ground integrated network, convex optimization theory, and game theory.

Kai Yu (Student Member, IEEE) received the B.S. degree in detection, guidance, and control technology from the University of Electronic Science and Technology of China, Chengdu, China, in 2019. He is currently pursuing the Ph.D. degree in communications and information system with Nanjing University, Nanjing, China. His research interests include resource allocation, machine learning for wireless communications, and heterogeneous cellular networks.

Quan Yu (Senior Member, IEEE) received the B.S. degree in information physics from Nanjing University, Nanjing, China, in 1986, the M.S. degree in radio wave propagation from Xidian University, Xi'an, China, in 1988, and the Ph.D. degree in fiber optics from the University of Limoges, Limoges, France, in 1992. He is a Research Fellow with the Peng Cheng Laboratory, Shenzhen, China. He was elected as a Fellow of the Chinese Academy of Engineering (CAE) for his contributions to the outstanding industrial engineering and practices of software radio and ad hoc networking in China, in 2009. He had won the First Prize of National Progress Awards in science and technology for his contribution to mobile ad hoc networking research and system integration, in 2007. He has been the Chairman of the Major Research Program on Space Information Networks of NSFC, since 2015. He was the General Co-Chair for the IEEE/CIC International Conference on Communications, China, in 2018, and the Technical Program Committee Vice-Chair of VTC Spring 2016. He is currently the Chair of the *Journal of Communications and Information Networks* (JCIN) Steering Committee. He is the Founding Editor-in-Chief of the JCIN.

Xuemin (Sherman) Shen (Fellow, IEEE) received the Ph.D. degree in electrical engineering from Rutgers University, New Brunswick, NJ, USA, in 1990.

He is currently a University Professor with the Department of Electrical and Computer Engineering, University of Waterloo, Waterloo, ON, Canada. His research focuses on network resource management, wireless network security, Internet of Things, 5G and beyond, and vehicular ad hoc and sensor networks. He is also a registered Professional Engineer of Ontario, Canada, an Engineering Institute of Canada Fellow, a Canadian Academy of Engineering Fellow, a Royal Society of Canada Fellow, and a Distinguished Lecturer of the IEEE Vehicular Technology Society and Communications Society.

Dr. Shen received the R. A. Fessenden Award in 2019 from the IEEE, Canada, James Evans Avant Garde Award in 2018 from the IEEE Vehicular Technology Society, Joseph LoCicero Award in 2015 and the Education Award in 2017 from the IEEE Communications Society. He has also received the Excellent Graduate Supervision Award in 2006 and the Outstanding Performance Award five times from the University of Waterloo and the Premier's Research Excellence Award (PREA) in 2003 from the Province of Ontario, Canada. He has served as the Technical Program Committee Chair/Co-Chair for the IEEE Globecom'16, the IEEE Infocom'14, the IEEE VTC'10 Fall, the IEEE Globecom'07, the Symposia Chair for the IEEE ICC'10, and the Chair for the IEEE Communications Society Technical Committee on Wireless Communications. He was the Editor-in-Chief of the IEEE INTERNET OF THINGS JOURNAL and the IEEE NETWORK and the Vice President on Publications of the IEEE Communications Society.